Bioconjugate Chemistry

Article

Cite This: *Bioconjugate Chem.* 2018, 29, 2232−2238

pubs.acs.org/bc

Polysarcosine as an Alternative to PEG for Therapeutic Protein Conjugation

Yali Hu,[†,‡] Yingqin Hou,[†] Hao Wang,[†] and Hua Lu*[,†]

[†]Beijing National Laboratory for Molecular Sciences, Center for Soft Matter Science and Engineering, Key Laboratory of Polymer Chemistry and Physics of Ministry of Education, College of Chemistry and Molecular Engineering and [‡]Peking-Tsinghua Center for Life Sciences, Academy for Advanced Interdisciplinary Studies, Peking University, Beijing 100871, China

Supporting Information

ABSTRACT: The performance of many therapeutic proteins, including human interferon-α2b (IFN), is often impeded by their intrinsic instability to protease, poor pharmacokinetics, and strong immunity. Although PEGylation has been an effective approach to improve the pharmacokinetics of many proteins, a few noticeable limitations have aroused vast research efforts in seeking alternatives to PEG for bioconjugation. Herein, we report our investigation on the use of polysarcosine (PSar), a nonionic and hydrophilic polypeptoid, for IFN modification. The site-specific conjugate PSar-IFN, generated by native chemical ligation in high yield, is systematically compared with a similarly produced PEG−interferon conjugate (PEG-IFN) to evaluate the in vitro and in vivo behaviors. PSar is found to show comparable ability in stabilizing IFN from protease digestion in vitro and prolonging the circulation half-life in vivo. Interestingly, PSar-IFN retains more activity in vitro and accumulates more in the tumor sites upon systemic administration than PEG-IFN. Most importantly, PSar-IFN is significantly more potent in inhibiting tumor growth and elicits considerably less anti-IFN antibodies in mouse than PEG-IFN. Together, our results demonstrate for the first time that PSar is an outstanding candidate for therapeutic protein conjugation. Considering the low toxicity, biodegradability, and excellent stealth effect of PSar, this study suggests that such polypeptoids hold enormous potential for many biomedical applications including protein delivery, colloidal stabilization, and nanomedicine.

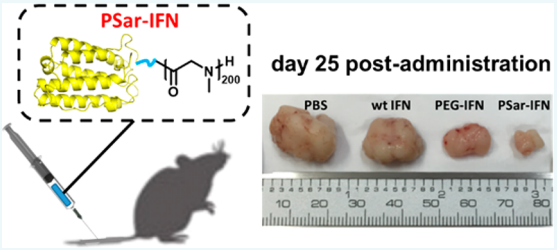

Downloaded via PEKING UNIV on July 19, 2018 at 06:14:37 (UTC).
See https://pubs.acs.org/sharingguidelines for options on how to legitimately share published articles.

INTRODUCTION

Protein−polymer conjugates are biohybrids in which the bioactive proteins are covalently modified with synthetic polymers. Presumably, the polymer conjugation can stabilize the therapeutic proteins from protease digestion, improve their pharmacokinetics in vivo, and sometimes enhance their activity.[1−3] Currently, all therapeutic protein−polymer conjugates on the market are based on poly(ethylene glycol) (PEG), the so-called PEGylation. Albeit effective, there is a growing awareness of a few intrinsic limitations of PEG including its nonbiodegradable backbone, reported patient hypersensitivity, and accelerated blood clearance (ABC effect).[4] This has stimulated vast research efforts in seeking alternatives to PEG for protein conjugation including poly(2-oxazoline)s,[5] polyglycerol,[6] zwitterionic polymers,[7] OEGylated poly(meth)acrylates,[8,9] and poly(amino acid)s.[10] Recently, polysarcosine (PSar), a polypeptoid based on the endogenous but nonproteinogenic amino acid sarcosine, has been considered an emerging "stealth" polymer for many biomedical applications.[11−14] In one sense, the nonionic and highly hydrophilic PSar can afford a large hydrodynamic volume and thus impart the desirable nonfouling character.[15] More interestingly, there has been accumulated evidence suggesting that the biodegradable PSar is more biocompatible and less immunogenic than PEG. For instance, PSar has been used to coat the surface of inorganic particles such as quantum dots and gold nanorods, which incurred less nonspecific interactions and systemic toxicity, preserved higher colloidal stability, and gave longer circulation time in vivo than the PEGylated ones.[16−18] PSar-conjugated Indocyanine Green (ICG), a small molecular photosensitizer for photoacoustic tumor imaging, has shown enhanced tumor accumulation and a higher signal/noise ratio in vivo as compared with a PEG-modified ICG analogue.[19] Copolymers containing PSar designed for peptide or protein encapsulation have preserved more activity than PEG did.[20,21] In light of these advances, we hypothesize that PSar is a promising material for therapeutic protein conjugation. Notably, although the conjugation of PSar to peptides has been nicely done,[22] the generation and systematic pharmacological evaluation of PSar-protein conjugate remains absent.

RESULTS AND DISCUSSION

Synthesis and Characterization. To test the hypothesis, we synthesized PSar-IFN, a *N*-terminal specific PSar-modified human interferon-α2b (IFN). IFN was selected because it was a therapeutic cytokine requiring PEGylation for longer circulating

Received: April 3, 2018
Revised: May 25, 2018
Published: June 4, 2018

© 2018 American Chemical Society

DOI: 10.1021/acs.bioconjchem.8b00237
Bioconjugate Chem. 2018, 29, 2232−2238

Scheme 1. Synthesis of PSar-IFN (A) and PEG-IFN (B)

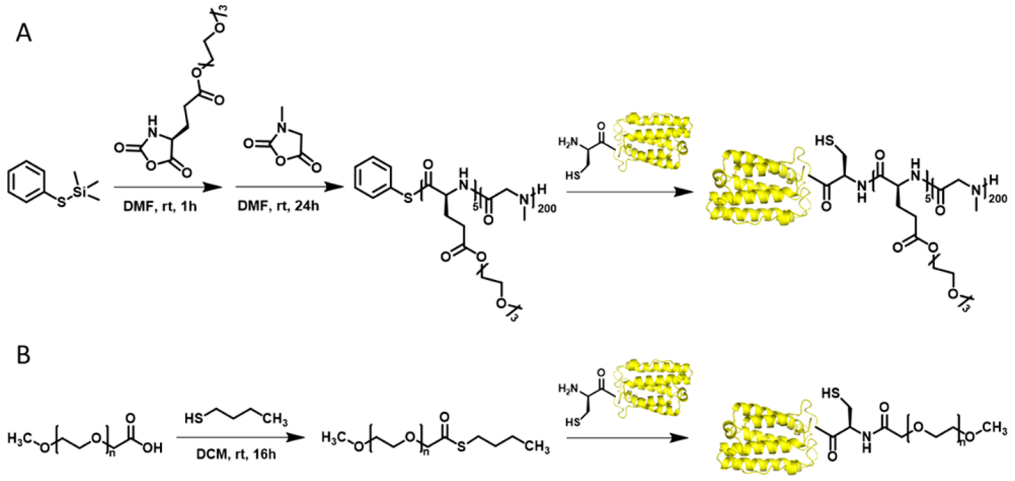

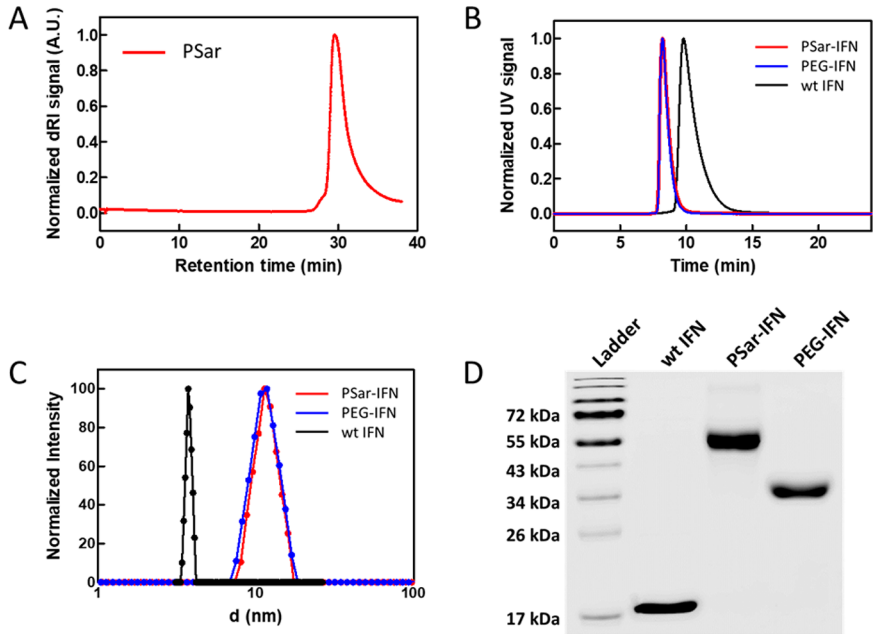

Figure 1. Characterization: (A) gel permeation chromatography of the polymer PhS-PSar, (B) size exclusion chromatography, (C) dynamic light scattering, and (D) SDS-PAGE electrophoresis of the two conjugates PSar-IFN and PEG-IFN.

half-life.[23] A *N*-terminal cysteine functionalized IFN mutant (Cys-IFN) was produced for native chemical ligation (NCL) following a previously reported method.[24] To generate PSar for Cys-IFN conjugation, we aimed to prepare a phenyl thioester-capped PSar via trimethylsilyl phenyl sulfide (PhS-TMS)-mediated ring-opening polymerization (ROP) of sarcosine *N*-carboxyanhydrides (SarNCA).[25] However, our initial attempts failed because PhS-TMS was unable to directly initiate the ROP of SarNCA, possibly due to the steric hindrance of the *N*-methyl group. To circumvent the problem, as shown in Scheme 1, we charged a small amount (5 equiv) of γ-(2-(2-(2-methoxyethoxy)ethoxy)ethoxy)esteryl L-glutamate *N*-Carboxyanhydride (EG_3GluNCA) to PhS-TMS (1 equiv) to extend a very short P(EG_3Glu) linker before the addition of SarNCA (200 equiv). This allowed the smooth growth of PSar after P(EG_3Glu) in one-pot and afforded the phenyl thioester-functionalized PSar (PhS-PSar). Gel permeation chromatography (GPC) and ^{1}H NMR characterization of PhS-PSar collectively indicated that the polymer had a molecular weight ~12 kDa with a polydispersity index (PDI) of 1.06 (Figures 1A and S1). Next, the *N*-terminal specific protein conjugate PSar-IFN was generated in high yield via the chemoselective NCL under a mild condition. To include a positive control, a PEGylated IFN (PEG-IFN) was produced via the same method by coupling a thioester-functionalized PEG (^{1}H NMR and MALDI available in Figure S2, PDI 1.04) and Cys-IFN (Scheme 1). We selected the 10 kDa PEG for conjugation because it has a comparable hydrodynamic radius with our PSar of 12 kDa.[26] Size exclusion chromatography (SEC) analysis of the two conjugates gave the same elution time, suggesting the two conjugates shared a similar hydrodynamic volume (Figure 1B). This notion was also well supported by the dynamic light scattering (DLS) measurement, which gave a 12.6 ± 0.7 and 12.8 ± 0.4 nm diameter for PSar-IFN and PEG-IFN, respectively (Figure 1C). SDS-PAGE gel analysis confirmed the successful generation and high purity of the two conjugates (Figure 1D). Interestingly, the apparent MW of both PEG-IFN and PSar-IFN, indicated by the protein ladder in the SDS-

DOI: 10.1021/acs.bioconjchem.8b00237
Bioconjugate Chem. 2018, 29, 2232−2238

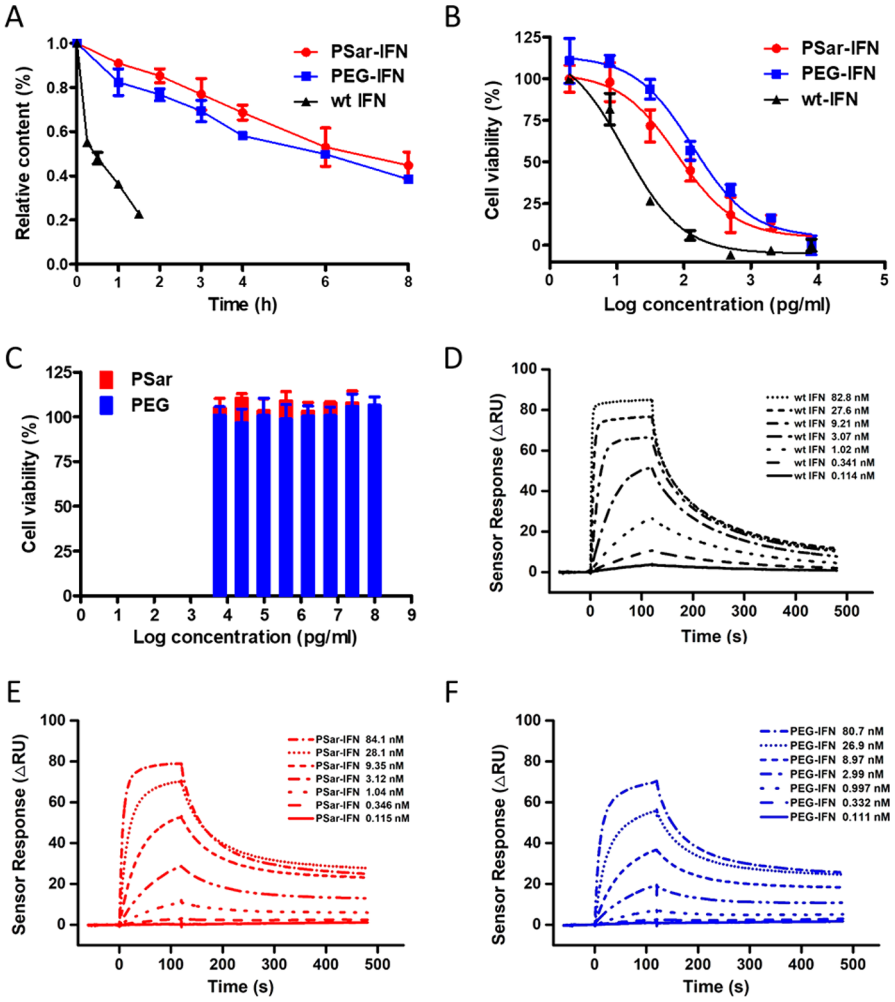

Figure 2. In vitro assessment of the conjugates: (A) trypsin digestion assay; (B and C) relative viabilities of Daudi cells treated with wt IFN, PSar-IFN, PEG-IFN (B), PSar, and PEG (C) for 48 h. Data are expressed as means ± SD (D–F) Surface plasmon resonance analysis of the binding of wt IFN (D), PSar-IFN (E), and PEG-IFN (F) to IFNAR2.

PAGE gel, did not agree well with their calculated sizes. Of note, such discrepancies were also frequently observed in the SDS-PAGE of other protein–polymer conjugates.[27] Apart from the MW, many other parameters including the chemical structure, polarity, and conformation of the polymers may alter their electrophoresis behaviors. Here, it was hypothesized that the rigidity difference of PEG and PSar (Kuhn length was 1.5 nm for PSar while 1.1 nm for PEG)[28] may affect the migration of the corresponding conjugates in the PAGE gel.

In Vitro Activity. To investigate the protease resistance and thermostability of the conjugates, we performed trypsin digestion and thermofluor assays. Compared with the wild type IFN (wt IFN) that was digested by trypsin rapidly within 2 h, both conjugates showed significantly enhanced stability under the same condition, with ~50% conjugates remain intact ~8 h after the treatment (Figures 2A and S3). Thermofluor assay revealed that the melting temperature (T_m) of the two conjugates were comparable with wt IFN, suggesting both PEG and PSar had very few influence to the thermostability of IFN (Figure S4). To test the antiproliferation activity of the two IFN conjugates, Daudi cells were incubated with the drugs at varied concentrations for 48 h. The half inhibition concentration (IC_{50}) of wt IFN, PSar-IFN, and PEG-IFN was found to be 13, 80, and 136 pg/mL, respectively (Figure 2B). This result indicated that PSar-IFN was slightly more potent than PEG-IFN. Notably, both PSar and PEG polymers were essentially nontoxic to Daudi cells (Figure 2C), implying that the cell killing ability of the conjugates was fully derived from the protein IFN. We further tested the binding affinity of the conjugates to the receptor of interferon-α2b (IFNAR2) by surface plasmon resonance (SPR) analysis (Figure 2D–F). The dissociation constant (K_D) was measured to be 1.07, 1.37, and 1.70 nM for wt IFN,[29,30] PSar-IFN, and PEG-IFN, respectively (Table 1). Moreover, it was found that the k_{on} was 5.04×10^6 and 2.04×10^6 M^{-1} s^{-1} for PSar-IFN and PEG-IFN, respectively. This result indicated that whereas the binding affinity of the two conjugates were comparable, PSar-IFN could associate with the receptor molecule more rapidly than PEG-IFN, which might explain the toxicity difference shown in Figure 2B.

Table 1. Surface Plasmon Resonance Analysis of the Binding of wt IFN, PSar-IFN, and PEG-IFN to IFNAR2

	k_{on} (M^{-1} s^{-1})	k_{off} (s^{-1})	K_D (M)
wt IFN	1.57×10^7	1.67×10^{-2}	1.07×10^{-9}
PSar-IFN	5.04×10^6	6.92×10^{-3}	1.37×10^{-9}
PEG-IFN	2.04×10^6	3.47×10^{-3}	1.70×10^{-9}

DOI: 10.1021/acs.bioconjchem.8b00237
Bioconjugate Chem. 2018, 29, 2232–2238

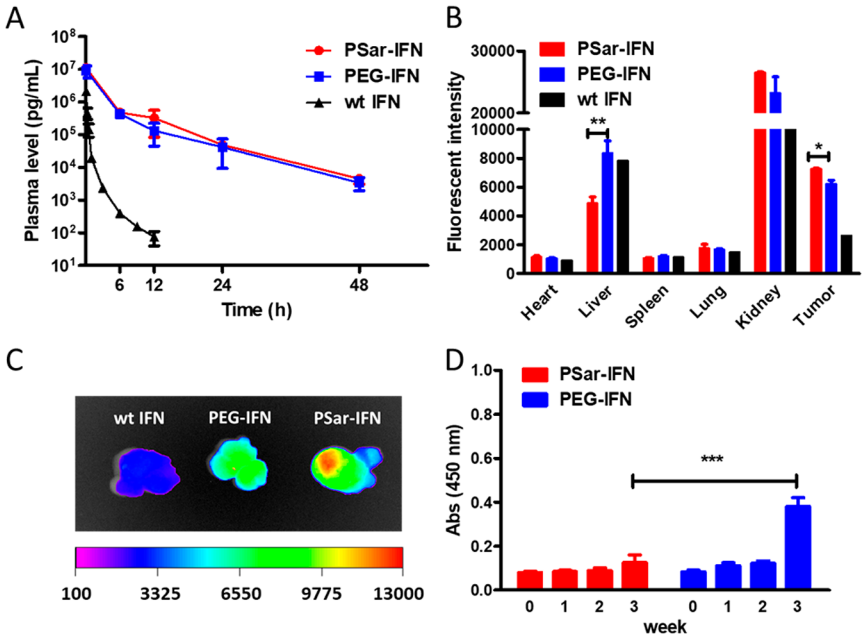

Figure 3. In vivo pharmacological evolution of the conjugates: (A) plasma IFN concentration at varied time points; (B) biodistribution at 24 h estimated by the fluorescence intensity of the extracted tissues; (C) fluorescent images of tumors at 24 h; (D) development of anti-IFN IgG at different times after weekly administration of the conjugates. Data are expressed as means ± SD: *p < 0.05, **p < 0.01, ***p < 0.001.

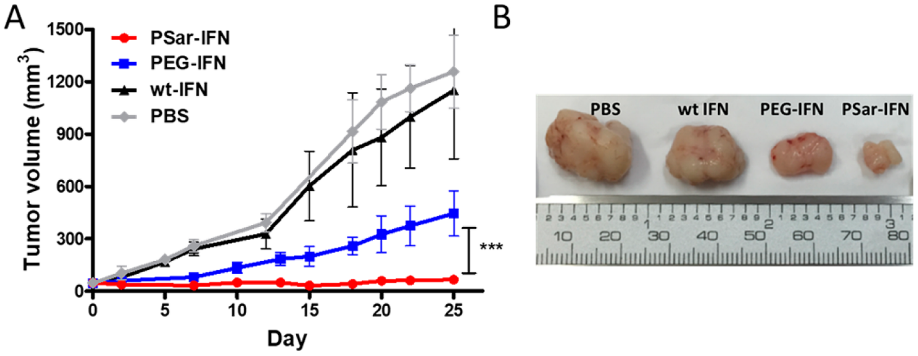

Figure 4. Antitumor efficacy of the conjugates on OVCAR3 tumor-bearing mice. (A) Tumor growth inhibition curve. Data are expressed as means ± SD, *** p < 0.001. (B) Images of the extracted tumors on day 25.

Pharmacokinetics, Biodistribution, and Immunogenicity. Next, we examined the performance of the conjugates in live animals. To analyze the pharmacokinetics (PK), wt IFN and the two conjugates were intravenously injected into Sprague−Dawley (SD) rats and the plasma IFN levels at different time points were measured by enzyme-linked immunosorbent assay (ELISA). The measured elimination half-life of wt IFN was almost equally extended from ∼0.8 h to ∼4.8 and 4.6 h for PSar-IFN and PEG-IFN, respectively (Figure 3A). To explore the biodistribution of different conjugates, all IFN variants were labeled with Cy5 (Figure S5) and injected intravenously into BALB/c nude mice bearing OVCAR3 tumors. The major organs and tumors were extracted 24 h after administration and analyzed with an in vivo imaging equipment. It was found that kidney was the brightest organ for all IFN variants, suggesting that renal clearance was the major elimination route (Figure 3B). This was not surprising considering the size of the conjugates shown in DLS (Figure 1C). Apart from the kidney, liver and tumor also displayed considerably higher fluorescence intensities than other organs including the heart, spleen, and lung. Compared with PEG-IFN, interestingly, PSar-IFN was shown to accumulate more in the tumor (p value <0.05) and have less exposure in the liver (p value <0.01) (Figure 3B and C). To evaluate the ability of the polymers in shielding IFN from immune recognition, PSar-IFN and PEG-IFN were intravenously administrated to immune competent SD rats weekly (n = 4). ELISA analysis indicated that, upon repetitive administration, PSar-IFN elicited significantly less anti-IFN IgG in week 3 than those produced by PEG-IFN (Figure 3D). Overall, the results suggested that PSar was an excellent stealth polymer for protein modification.

Antitumor Efficacy. Finally, we evaluated the antitumor efficacy of the conjugates on OVCAR3 tumor-bearing BALB/c nude mice. On day 0, the mice with a mean tumor volume at 50 mm^3 were randomly assigned to four groups (n = 5−7). PSar-IFN, PEG-IFN, wt IFN, and PBS were infused at the same IFN dosage every 5 days. On day 25, the mean volume of tumor in the PBS group and the wt IFN group increased to over 1000 mm^3. In contrast, both PSar-IFN and PEG-IFN treatments showed conspicuously better tumor growth inhibition. Most importantly, mice in the PSar-IFN group were found to have appreciably smaller tumors than those in the PEG-IFN group

DOI: 10.1021/acs.bioconjchem.8b00237
Bioconjugate Chem. 2018, 29, 2232−2238

(Figure 4). This result clearly supported the argument of utilizing PSar as a conjugation partner for enhanced therapeutic efficacy of protein. Notably, no significant loss in weight was observed in the PSar-IFN group, suggesting the conjugate was well-tolerated at the current dose (Figure S6). The excellent biosafety profile of PSar-IFN was also illustrated by the histological examination of the dissected organ sections, which showed no major damage in the heart, liver, spleen, lung, and kidney (Figure S7).

CONCLUSIONS

In summary, we synthesized PSar-IFN, an *N*-terminal specific polysarcosine−interferon conjugate, and compared its activity in parallel with a PEG-modified IFN. Our results indicated that the similarly sized PSar-IFN and PEG-IFN possessed comparable protease resistance to trypsin digestion. Moreover, the two conjugates also exhibited a similarly improved circulation half-life in plasma. Interestingly, PSar-IFN was slightly more potent than PEG-IFN in inhibiting tumor cell proliferation in vitro, and accumulated more in tumor sites after systemic administration than PEG-IFN. Remarkably, PSar-IFN incurred less anti-IFN IgG in plasma after multiple administrations. The superior in vivo antitumor efficacy of PSar-IFN over PEG-IFN was confirmed by the tumor growth inhibition study. Taken together, our results demonstrated for the first time that PSar was an outstanding candidate for therapeutic protein conjugation. Considering the low toxicity, biodegradability, and excellent stealth effect of PSar, the present work suggested that such polypeptoids had enormous potential for many biomedical applications including protein delivery, colloidal stabilization, and nanomedicine.

EXPERIMENTAL SECTION

Materials. Sarcosine was purchased from Aladdin (Shanghai, China). Phenyl trimethylsilyl sulfide (PhS-TMS) was purchased from Sigma-Aldrich (St. Louis, USA). Methoxy PEG Carboxyl (mPEG-COOH, MW 10 kDa) was purchased from JenKem Technology Co., Ltd. (Beijing, China). Butanethiol was purchased from Energy Chemical (Shanghai, China). Cy5 was purchased from ApexBio (Houston, USA). CellTiter-Blue was purchased from Promega (Madison, USA). IFNAR2 was purchased from Sino Biological Inc. (Beijing, China). IFN alpha human matched antibody pair was purchased from eBiosciense (California, USA). Wild type and mutant IFNs, TEV protease were produced according to protocols reported elsewhere.[31] γ-(2-(2-(2-Methoxyethoxy)ethoxy)ethoxy)esteryl L-glutamate *N*-Carboxyanhydride (EG_3GluNCA)[32] and Sarcosine *N*-Carboxyanhydride (SarNCA) were obtained in accordance with established methods.[33]

Instrument. Gel permeation chromatography (GPC) characterization was performed on tandem columns (500 Å, 10^3 Å, 10^4 Å Phenogel columns, 5 μm, 7.8 × 300 mm^2, Phenomenex, Torrance, CA) at 50 °C using DMF with 0.1 M LiBr as the mobile phase. The molecular weight (MW) of PSar was calculated based on a d*n*/d*c* value reported previously.[34] NMR spectra were analyzed on ARX400 (Bruker Co., Germany). Mass spectrum was recorded on a MALDI-TOF (AB Sciex TOF 5800, CA). Protein purification was performed on ÄKTA pure (GE, USA) using Mono S 5/50 GL column or Superdex 75 10/300 GL column. Dynamic light scattering (DLS) examinations were recorded on a Nanobrook Omni at 25 °C (Brookhaven Instrument Corp. USA). SDS-PAGE gel was imaged on typhoon FLA 9500 (GE, USA). Protein concentration was determined by NanoPhotometer P330 (Implen, Germany). The viability assay and ELISA were recorded on multimode plate reader (PerkinElmer, USA). Thermofluor assay was performed on LightCycler 96 (Roche, Switzerland). Surface plasmon resonance (SPR) analysis was performed on Biacore T200 (GE, USA). Biodistributions of the conjugates were imaged by FX Pro (Kodak, USA). The histologic sections were imaged on Vectra (Caliper, USA).

Cell Lines and Animals. Human cell line Daudi, obtained from China Infrastructure of Cell Line Resource, was grown in RPMI 1640 with L-glutamine (Cellgro, USA) with 20% FBS (Gibco, USA), 100 IU penicillin, and 100 μg/mL streptomycin (Cellgro, USA). Human ovarian carcinoma OVCAR3 was cultured in RPMI 1640 with L-glutamine supplemented with 20% FBS (PAN, Germany), 100 IU penicillin, 100 μg/mL streptomycin (Cellgro, USA), and 0.01 mg/mL insulin from bovine (SIGMA, USA). Female SD rats and female BALB/c nude mice were purchased from Vital River Laboratories (Beijing, China). All the in vivo experiments were carried out with the permission of the experimental animal ethics committee.

Synthesis of PhS-PSar. In a glovebox, EG_3GluNCA (6.9 mg, 0.022 mmol, 5.0 equiv) in anhydrous DMF (60 μL) was added to PhS-TMS (8.7 μL × 0.5 M, 1.0 equiv) and stirred for 1 h at room temperature. SarNCA (100 mg, 0.87 mmol, 200.0 equiv) was added to the mixture and stirred for another 48 h at room temperature. The polymer was precipitated in anhydrous ether (100 mL), centrifuged at 4000 *g* for 5 min, and the sediment was redissolved in ultrapure H_2O and further purified by a PD 10 desalting column (GE, USA). The collected polymer solution was freeze-dried to yield a fluffy powder (52 mg, 85%).

Synthesis of the Thioester Capped PEG. mPEG-COOH (200 mg, MW 10 kDa) was dissolved in CH_2Cl_2 (2 mL), to which was added DCC (74 mg) and butanethiol (80 μL). The reaction was stirred overnight at room temperature. The polymer was precipitated in anhydrous ether (100 mL), centrifuged at 4000 *g* for 5 min, and the sediment was redissolved in ultrapure H_2O and further purified by a PD 10 desalting column (GE, USA). The collected polymer solution was freeze-dried to yield a fluffy powder (165 mg, yield 82%).

General Protocol for the Synthesis of PSar-IFN and PEG-IFN. Cys-IFN was produced by TEV protease digestion and concentrated to ∼5 mg/mL. Typically, Cys-IFN (4.5 mg/mL × 1 mL, 1.0 equiv) in Tris-HCl buffer was added PhS-PSar powder (6.8 mg, 3.0 equiv). The mixture was incubated at room temperature for ∼8 h, during which the smell of phenylthiol could be noticed. Purification was performed by passing the diluted mixture through a PD 10 desalting column to remove all small molecular impurities, and followed by a Mono S column on FPLC (Buffer A: 50 mM CH_3COONa, pH 4.5; Buffer B: 50 mM CH_3COONa with 2 M NaCl, pH 4.5). Cy5 labeling of the conjugate was performed by following the same protocol reported elsewhere.[24] Endotoxin was removed by passing the conjugate solution through an endotoxin affinity column before animal studies. PEG-IFN was synthesized and purified by following the same protocol.

Trypsin Digestion Assay. wt IFN, PEG-IFN, and PSar-IFN were diluted to 10 μM in Tris-HCl buffer, mixed with isometric 0.1 μM trypsin, and then incubated at 37 °C. At selected time points, each sample in triplicate was boiled at 98 °C for 10 min to terminate the digestion. All trypsin-digested

DOI: 10.1021/acs.bioconjchem.8b00237
Bioconjugate Chem. 2018, 29, 2232−2238

samples at different time points were analyzed on one SDS-PAGE gel together. Degradation of the conjugates at each time point was determined by the relative coomassie blue staining signal intensity and quantitatively analyzed through typhoon.

Thermofluor Assay. The thermostability of all samples were performed on LightCycler 96 (Roche, Switzerland). Briefly, 5 μM conjugates and 20 × Sypro orange protein stain (both are final concentrations) in PBS were added into an opaque white 96-well plate with temperature varied from 37 to 98 °C and detected the change of fluorescence intensities. T_m was analyzed by the LightCycler 96 SW 1.1.

Surface Plasmon Resonance (SPR) Analysis. Binding affinities to receptor were performed on Biacore T200 using CM5 sensor at 25 °C. The IFNAR2 was diluted into 10 mM NaOAc buffer pH 5.0 at a concentration of 50 ug/mL and covalently attached to the surface of the sensor via NHS-amine chemistry. Analyses of the interactions between the IFN variants with IFNAR2 were performed in HBS-EP+ buffer (10 mM HEPES, 150 mM NaCl, 3 mM EDTA, 0.05% v/v surfactant P20, pH 7.4) at a flow rate of 30 μL/min. Seven different concentrations were measured for each sample. Between measurements, 10 mM glycine-HCl (pH 3.0) was used for chip regeneration. The results were analyzed by BIA evaluation software and fitted with one to one kinetic model.

Cytotoxicity Assay. PhS-PSar, PEG-thioester or wt IFN, PSar-IFN, PEG-IFN were added into a black 96-well plate at gradient concentrations which seeded 5000 Daudi cells per well and incubated for 48 h (n = 3). The relative viabilities were detected by CellTiter-Blue (Promega, USA).

Pharmacokinetics Assay. Female SD rats weighing ∼250 g were randomly assigned to three groups (n = 2 or 3). wt IFN, PSar-IFN, or PEG-IFN was intravenously injected to the rats at a 0.2 mg IFN/kg dose. At predetermined time points, the plasma were acquired from orbit followed by centrifugation. The concentration of IFN in each plasma sample was evaluated by ELISA and data were processed by GraphPad Prism 5.0.

In Vivo Biodistribution. OVCAR3 cells (1.0×10^7) suspended in RPMI 1640 were mixed with isometric matrigel and subcutaneously inoculated into 6-weeks-old BALB/c nude mice. The mice were randomly assigned to three groups (n = 2) while the tumors grew to ∼250 mm^3 and were injected with Cy5-marked PSar-IFN, PEG-IFN, or wt IFN at 20 μg IFN/mouse via the tail vein. The mice were anaesthetized by chloral hydrate to extract major organs and tumors 24 h after the drug infusion. The organs and tumors were recorded on FX Pro (Kodak, USA) and the biodistribution was assessed based on the fluorescent intensity.

Immunogenicity Assay. Female SD rats were randomly assigned to two groups (n = 4) on day 1 and infused with PSar-IFN or PEG-IFN (100 ng IFN each) through tail vein under anesthetic conditions. The same administration was repeated on days 8 and 15. Before each injection, blood were collected on day 1, 8, 15, and 22. The anti-IFN IgG levels in the sera were then evaluated by ELISA.

In Vivo Antitumor Efficacy. OVCAR3 cells (1.0×10^7) suspended in RPMI 1640 were mixed with isometric matrigel and subcutaneously inoculated into 6-week-old BALB/c nude mice. The mice were randomly assigned to four groups (n = 5−7) while the tumors grew to ∼50 mm^3, and received PBS, wt IFN, PEG-IFN, or PSar-IFN treatment at a 10 μg IFN/mouse dose via the tail vein route once every 5 days. The volume of tumor was acquired through the following formula: $V = L \times W^2/2$. Experimental results were processed using GraphPad Prism 5.0.

Histopathology Evaluation. On day 25, the mice were executed to extract the tumors and major organs such as heart, liver, spleen, lung, and kidney for cut into slices and stained with hematoxylin and eosin (H&E), which were then imaged on Vectra.

■ ASSOCIATED CONTENT

Supporting Information

The Supporting Information is available free of charge on the ACS Publications website at DOI: 10.1021/acs.bioconjchem.8b00237.

^{1}H NMR, MALDI, SDS-PAGE, thermal denaturation curves, relative weight of mice, histopathology evaluation (PDF)

■ AUTHOR INFORMATION

Corresponding Author

*E-mail: chemhualu@pku.edu.cn.

ORCID

Hua Lu: 0000-0003-2180-3091

Notes

The authors declare no competing financial interest.

■ ACKNOWLEDGMENTS

This work was financially supported by National Key Research and Development Program of China (2016YFA0201400). We thank the grants from National Natural Science Foundation of China (21722401, 21474004, and 21434008). H.L. thanks the startup funding from Youth Thousand-Talents Program of China. We thank the protein interaction facility of School of Life Sciences, Peking University, and Dr. Hui Li for help with SPR analysis.

■ REFERENCES

(1) Říhová, B., Jelínková, M., Strohalm, J., Šubr, V., Plocová, D., Hovorka, O., Novák, M., Plundrová, D., Germano, Y., and Ulbrich, K. (2000) Polymeric drugs based on conjugates of synthetic and natural macromolecules.: II. Anti-cancer activity of antibody or (Fab′)2-targeted conjugates and combined therapy with immunomodulators. *J. Controlled Release 64*, 241−261.

(2) Pasut, G., and Veronese, F. M. (2012) State of the art in PEGylation: the great versatility achieved after forty years of research. *J. Controlled Release 161*, 461−472.

(3) Hu, J., Wang, G., Zhao, W., and Gao, W. (2016) In situ growth of a C-terminal interferon-alpha conjugate of a phospholipid polymer that outperforms PEGASYS in cancer therapy. *J. Controlled Release 237*, 71−77.

(4) Pelegri-O'Day, E. M., Lin, E.-W., and Maynard, H. D. (2014) Therapeutic Protein−Polymer Conjugates: Advancing Beyond PEGylation. *J. Am. Chem. Soc. 136*, 14323−14332.

(5) Mero, A., Fang, Z., Pasut, G., Veronese, F. M., and Viegas, T. X. (2012) Selective conjugation of poly(2-ethyl 2-oxazoline) to granulocyte colony stimulating factor. *J. Controlled Release 159*, 353−361.

(6) Thomas, A., Müller, S. S., and Frey, H. (2014) Beyond Poly(ethylene glycol): Linear Polyglycerol as a Multifunctional Polyether for Biomedical and Pharmaceutical Applications. *Biomacromolecules 15*, 1935−1954.

(7) Keefe, A. J., and Jiang, S. (2012) Poly(zwitterionic)protein conjugates offer increased stability without sacrificing binding affinity or bioactivity. *Nat. Chem. 4*, 59−63.

DOI: 10.1021/acs.bioconjchem.8b00237
Bioconjugate Chem. 2018, 29, 2232−2238

(8) Hu, J., Wang, G., Zhao, W., Liu, X., Zhang, L., and Gao, W. (2016) Site-specific in situ growth of an interferon-polymer conjugate that outperforms PEGASYS in cancer therapy. *Biomaterials 96*, 84−92.
(9) Nguyen, T. H., Kim, S.-H., Decker, C. G., Wong, D. Y., Loo, J. A., and Maynard, H. D. (2013) A heparin-mimicking polymer conjugate stabilizes basic fibroblast growth factor. *Nat. Chem. 5*, 221−227.
(10) Lu, H., Wang, J., Song, Z., Yin, L., Zhang, Y., Tang, H., Tu, C., Lin, Y., and Cheng, J. (2014) Recent advances in amino acid N-carboxyanhydrides and synthetic polypeptides: chemistry, self-assembly and biological applications. *Chem. Commun. 50*, 139−155.
(11) Lau, K. H. A., Ren, C., Sileika, T. S., Park, S. H., Szleifer, I., and Messersmith, P. B. (2012) Surface-Grafted Polysarcosine as a Peptoid Antifouling Polymer Brush. *Langmuir 28*, 16099−16107.
(12) Chan, B. A., Xuan, S., Li, A., Simpson, J. M., Sternhagen, G. L., Yu, T., Darvish, O. A., Jiang, N., and Zhang, D. (2018) Polypeptoid polymers: Synthesis, characterization, and properties. *Biopolymers 109*, e23070.
(13) Birke, A., Ling, J., and Barz, M. (2018) Polysarcosine-containing copolymers: Synthesis, characterization, self-assembly, and applications. *Prog. Polym. Sci. 81*, 163−208.
(14) Sela, M., and Arnon, R. (1960) Studies on the chemical basis of the antigenicity of proteins. 3. The role of rigidity in the antigenicity of polypeptidyl gelatins. *Biochem. J. 77*, 394−399.
(15) Tao, X., Deng, C., and Ling, J. (2014) PEG-Amine-Initiated Polymerization of Sarcosine N-Thiocarboxyanhydrides Toward Novel Double-Hydrophilic PEG-b-Polysarcosine Diblock Copolymers. *Macromol. Rapid Commun. 35*, 875−881.
(16) Zhu, H., Chen, Y., Yan, F.-J., Chen, J., Tao, X.-F., Ling, J., Yang, B., He, Q.-J., and Mao, Z.-W. (2017) Polysarcosine brush stabilized gold nanorods for in vivo near-infrared photothermal tumor therapy. *Acta Biomater. 50*, 534−545.
(17) Fokina, A., Klinker, K., Braun, L., Jeong, B. G., Bae, W. K., Barz, M., and Zentel, R. (2016) Multidentate Polysarcosine-Based Ligands for Water-Soluble Quantum Dots. *Macromolecules 49*, 3663−3671.
(18) Chen, Y., Xu, Z., Zhu, D., Tao, X., Gao, Y., Zhu, H., Mao, Z., and Ling, J. (2016) Gold nanoparticles coated with polysarcosine brushes to enhance their colloidal stability and circulation time in vivo. *J. Colloid Interface Sci. 483*, 201−210.
(19) Sano, K., Ohashi, M., Kanazaki, K., Makino, A., Ding, N., Deguchi, J., Kanada, Y., Ono, M., and Saji, H. (2017) Indocyanine Green -Labeled Polysarcosine for in Vivo Photoacoustic Tumor Imaging. *Bioconjugate Chem. 28*, 1024−1030.
(20) Weber, B., Kappel, C., Scherer, M., Helm, M., Bros, M., Grabbe, S., and Barz, M. (2017) PeptoSomes for Vaccination: Combining Antigen and Adjuvant in Polypept(o)ide-Based Polymersomes. *Macromol. Biosci. 17*, 1700061.
(21) Hsiao, L. W., Lai, Y. D., Lai, J. T., Hsu, C. C., Wang, N. Y., Wang, S. S., and Jan, J. S. (2017) Cross-linked polypeptide-based gel particles by emulsion for efficient protein encapsulation. *Polymer 115*, 261−272.
(22) Klinker, K., Holm, R., Heller, P., and Barz, M. (2015) Evaluating chemical ligation techniques for the synthesis of block copolypeptides, polypeptoids and block copolypept(o)ides: a comparative study. *Polym. Chem. 6*, 4612−4623.
(23) Chawla-Sarkar, M., Lindner, D. J., Liu, Y.-F., Williams, B. R., Sen, G. C., Silverman, R. H., and Borden, E. C. (2003) Apoptosis and interferons: Role of interferon-stimulated genes as mediators of apoptosis. *Apoptosis 8*, 237−249.
(24) Hou, Y. Q., Yuan, J. S., Zhou, Y., Yu, J., and Lu, H. (2016) A Concise Approach to Site-Specific Topological Protein-Poly(amino acid) Conjugates Enabled by in Situ-Generated Functionalities. *J. Am. Chem. Soc. 138*, 10995−11000.
(25) Yuan, J., Sun, Y., Wang, J., and Lu, H. (2016) Phenyl Trimethylsilyl Sulfide-Mediated Controlled Ring-Opening Polymerization of α-Amino Acid N-Carboxyanhydrides. *Biomacromolecules 17*, 891−896.
(26) Huesmann, D., Sevenich, A., Weber, B., and Barz, M. (2015) A head-to-head comparison of poly(sarcosine) and poly(ethylene glycol) in peptidic, amphiphilic block copolymers. *Polymer 67*, 240−248.
(27) Yun, Q., Xing, W., Ma, G., and Su, Z. (2006) Preparation and characterization of mono-PEGylated consensus interferon by a novel polyethylene glycol derivative. *J. Chem. Technol. Biotechnol. 81*, 776−781.
(28) Weber, B., Birke, A., Fischer, K., Schmidt, M., and Barz, M. (2018) Solution Properties of Polysarcosine: From Absolute and Relative Molar Mass Determinations to Complement Activation. *Macromolecules 51*, 2653−2661.
(29) Zhang, B., Xu, H., Chen, J., Zheng, Y., Wu, Y., Si, L., Wu, L., Zhang, C., Xia, G., Zhang, L., and Zhou, D. (2015) Development of next generation of therapeutic IFN-α2b via genetic code expansion. *Acta Biomater. 19*, 100−111.
(30) Schmeisser, H., Gorshkova, I., Brown, P. H., Kontsek, P., Schuck, P., and Zoon, K. C. (2007) Two Interferons Alpha Influence Each Other during Their Interaction with the Extracellular Domain of Human Type Interferon Receptor Subunit 2. *Biochemistry 46*, 14638−14649.
(31) Hou, Y., Zhou, Y., Wang, H., Wang, R., Yuan, J., Hu, Y., Sheng, K., Feng, J., Yang, S., and Lu, H. (2018) Macrocyclization of Interferon−Poly(α-amino acid) Conjugates Significantly Improves the Tumor Retention, Penetration, and Antitumor Efficacy. *J. Am. Chem. Soc. 140*, 1170−1178.
(32) Chen, C., Wang, Z., and Li, Z. (2011) Thermoresponsive Polypeptides from Pegylated Poly-l-glutamates. *Biomacromolecules 12*, 2859−2863.
(33) Fetsch, C., Grossmann, A., Holz, L., Nawroth, J. F., and Luxenhofer, R. (2011) Polypeptoids from N-Substituted Glycine N-Carboxyanhydrides: Hydrophilic, Hydrophobic, and Amphiphilic Polymers with Poisson Distribution. *Macromolecules 44*, 6746−6758.
(34) Cui, S., Pan, X., Gebru, H., Wang, X., Liu, J., Liu, J., Li, Z., and Guo, K. (2017) Amphiphilic star-shaped poly(sarcosine)-block-poly(ε-caprolactone) diblock copolymers: one-pot synthesis, characterization, and solution properties. *J. Mater. Chem. B 5*, 679−690.

DOI: 10.1021/acs.bioconjchem.8b00237
Bioconjugate Chem. 2018, 29, 2232−2238